Journal of Glaciology

Letter

Cite this article: Kavan J, Haagmans V (2021). Seasonal dynamics of snow ablation on selected glaciers in central Spitsbergen derived from Sentinel-2 satellite images. *Journal of Glaciology* **67**(265), 961–966. https://doi.org/10.1017/jog.2021.36

Received: 5 October 2020
Revised: 8 March 2021
Accepted: 9 March 2021
First published online: 13 April 2021

Keywords:
Glacier ablation phenomena; glacier mass balance; snow; wind-blown snow

Author for correspondence:
Jan Kavan,
E-mail: jan.kavan.cb@gmail.com

cambridge.org/jog

Seasonal dynamics of snow ablation on selected glaciers in central Spitsbergen derived from Sentinel-2 satellite images

Jan Kavan[1] and Vincent Haagmans[2]

[1]Polar-Geo-Lab, Department of Geography, Faculty of Science, Masaryk University, Brno, Czechia and [2]Institute of Environmental Engineering, ETH Zurich, Zurich, Switzerland

Abstract

The dynamics of seasonal snow ablation on six glaciers in central Spitsbergen (Dicksonland) were assessed by examining a set of Sentinel-2 satellite images covering the summer ablation season for the period 2016–19. All glaciers lost 80% or more of their surface snow cover during the studied ablation seasons. This bolsters the recently observed trend of local glacier thinning, even at higher altitudes. Snow ablation dynamics are highly dependent on the glaciers altitudes, their position relative to the prevailing wind direction and the exposure to insolation. The accumulation areas of the studied glaciers were delimited based on the overlap of the minimum extent of snow-covered areas in the four consecutive studied summer seasons. The high temporal and spatial resolutions of available images enabled a detailed description of the seasonal snow ablation dynamics. Moreover, an estimate of the average number of days with below threshold glacier snow cover was made. This study contributes to our understanding of recent processes and might further support the modelling of glacier melt and subsequent runoff.

Introduction

Svalbard is experiencing dramatic cryospheric changes comprising permafrost thaw (Humlum and others, 2003) and glacier retreat (Nuth and others, 2007; Schuler and others, 2020). In central Spitsbergen, on the main island of the Svalbard archipelago, glaciers are retreating since the termination of the Little Ice Age (Martń-Moreno and others, 2017), dated here around 1900 CE (Szczuciński and others, 2009). West of Petunia Bay in central Spitsbergen, small valley glaciers have retreated significantly, especially in the second half of the 20th century (e.g. Rachlewicz and others, 2007; Kavan, 2020). This contrasts with the glaciers on the eastern side of the Petunia Bay that are fed by the vast Lomonosov ice cap. Their areal retreat is negligible in comparison with the valley glaciers on the western side of the bay. Małecki (2016) identified that these retreating valley glaciers have been melting even in the high elevated areas that used to be the accumulation zones of the glaciers. Such small glaciers seem to be more sensitive to climate fluctuations in terms of their areal extent as well as volume (see Lapazaran and others, 2013; Ai and others, 2014; Marlin and others, 2017). Noël and others (2020) demonstrated that only a modest atmospheric warming drastically reduced the proportion of firn zone essential for mass accumulation, and increased runoff from the exposed glacier surface.

Snow accumulation combined with above zero temperatures are crucial factors governing a glacier mass balance. Whereas the air temperature is rather spatially homogeneous, the snow accumulation is driven mainly by topography and can differ significantly according to the local prevailing wind flow and relief (Jaedicke and Gauer, 2005). High snow accumulation during winter can be found on, for example, the high-elevated northern slopes of the Sven glacier (Małecki, 2015) included in this study. Currently, the assessment of seasonal snow cover based on remote sensing data is not a completely new approach (e.g. Turpin and others, 2000; Nolin, 2010). The increasing spatial and temporal resolutions of new, freely available satellite products is, however, making such assessments more valuable and relevant.

The study presented here aims to describe the seasonal ablation dynamics of the snow cover extent on six glaciers in Dicksonland, central Spitsbergen, based on Sentinel-2 satellite images from 2016 to 2019. By describing the extent of the snow cover during the ablation season, we aim to increase process understanding of the recently observed accelerated thinning of the studied glaciers (e.g. Małecki, 2016). Note that the spatial variability of snow on glaciers in central Spitsbergen was identified as an important knowledge gap by Gallet and others (2018), which the authors hope to partially fill. In addition, the goal is to identify accumulation areas of the studied glaciers where snow cover persists throughout the whole melting season and estimate during how many days on average the glacier snow cover is below a set threshold.

Study site

Six glaciers (Table 1) were chosen for the purpose of this study: Bertil (B), Ferdinand (F), Sven (S), Elsa (E), Austre Muninbreen (AM) and Vestre Muninbreen (VM). The six selected glaciers

Table 1. Basic characteristics of the studied glaciers (based on 2009 DEM and topography data)

Glacier	Area km^2	Min elevation m	Median elevation m	Max elevation m	Mean slope°	Dominant aspect
Bertil	3.77	230	500	730	10	South
Elsa	0.15	450	580	690	22	North
Ferdinand	0.67	240	420	540	15	East
Sven	3.69	170	480	740	10	East
Austre Munin	1.97	250	460	730	10	South-west
Vestre Munin	2.56	270	440	750	9	South

are located in central Spitsbergen, on the western side of the Petunia Bay (Fig. 1). All glaciers are of a valley type, except for Elsa glacier which is only a remnant of the former valley glacier and has all the characteristics of a cirque glacier. The glaciers used to be considered polythermal (Rachlewicz and others, 2007). However, their small depth revealed from ground penetrating radar (GPR) surveys (Małecki, 2013; Procházková and others, 2019) and their physical surface characteristics reflect more likely cold based glaciers or glaciers in transition (Mallinson and others, 2019).

Central Spitsbergen experiences a rather dry continental climate characterised by low winter and high summer temperatures in comparison with other parts of Svalbard (Gjelten and others, 2016). Przybylak and others (2014) determined the study area and Nordaustlandet as the most continental regions of Svalbard in terms of all three examined parameters – annual range of air temperature, thermal climate continentality index and thermal oceanity index. The mean annual air temperature in the Petunia Bay was −3.7°C for the period 2013–15, with a maximum of 17°C in July 2015 and a minimum of −28.3°C in February 2015 (Ambrožvá and Láska, 2017). The annual average precipitation is estimated to be around 250 mm in recent years as measured at the Svalbard airport weather station, the closest precipitation record available (NPI, 2021). The continental character of the local climate is enforced by its distance from the open sea and the long persistence of the sea-ice cover (Nilsen and others, 2008). However, this may change with the ongoing increase of air and sea water temperatures and consequent sea-ice extent reduction.

Materials and methods

Sentinel-2 satellite images were obtained from the Sentinel Hub (https://www.sentinel-hub.com) Earth Observation Browser. Available images covering the assumed ablation season (1 June–30 September) with cloud coverage smaller than 20% were selected from the database and checked for their suitability. As a result, 14 images for 2016, 13 for 2017, 14 for 2018 and 18 images for 2019 (list of images is provided in the Table 4 - Appendix) could be obtained. These false colour images (bands 8, 4, 3) were downloaded as georeferenced TIFF files and processed in ArcGIS software to manually delimit the snow cover on the glaciers. The bright areas in Figure 1b on the false colour image distinctively characterise the remaining snow cover on the glacier surface in the middle of the ablation season.

The minimum extent of snow cover was manually delimited for each of the 4 years that were investigated and consecutively overlapped to estimate the accumulation areas of the studied glaciers. Note that the snow coverage for Vestre Muninbreen (VM) in 2016 was derived from an image dated to 3 August 2016. Yet, minimum snow cover extent very likely occurred at a later point in time, similar to the five other studied glaciers. For the latter glaciers, the minimum snow cover extent was extracted from an image dated to 23 August 2016 since on this date the cloud cover over a VM inhibited the definition of the snow cover extent. A similar situation occurred on 13 August 2016 for both Austre Muninbreen (AM) and VM.

In addition to the minimum snow cover extent, the period during which no protective layer of snow is available on a significant part of the glacier is of relevance for the mass balance. Therefore, a linear interpolation with a daily time step was applied to the discontinuous records of snow cover extent. Consequently, the number of days were counted for which a snow cover below a defined threshold (10, 30, 50, 70, 90%) existed. These estimates were then transformed into an average over the study period for each glacier. A Digital Elevation Model (DEM) from 2009 (id 13822) provided by the Norwegian Polar Institute (NPI) was used to assess the hypsometry of the studied glaciers and to derive their basic characteristics (Table 1). Glacier outlines from topographic data (NPI database) derived from 2009 aerial images were used.

Results

Similar snow cover ablation dynamics were found for the six investigated glaciers during the study period, see Figure 2.

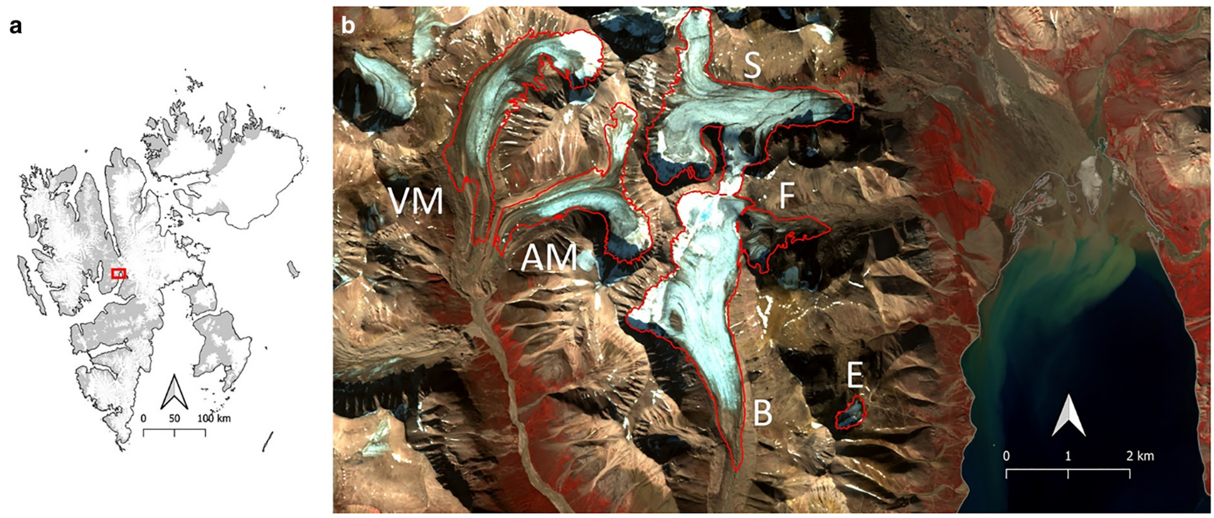

Fig. 1. (a) Location of the study area on Svalbard and (b) Sentinel-2 image of the study area (false colour, bands 8, 4, 3) from 28 July 2019 used for delineation of snow coverage on selected glaciers; glacier outlines of the six glaciers studied marked with their abbreviations: Bertil (B), Ferdinand (F), Sven (S), Elsa (E), Austre Muninbreen (AM) and Vestre Muninbreen (VM).

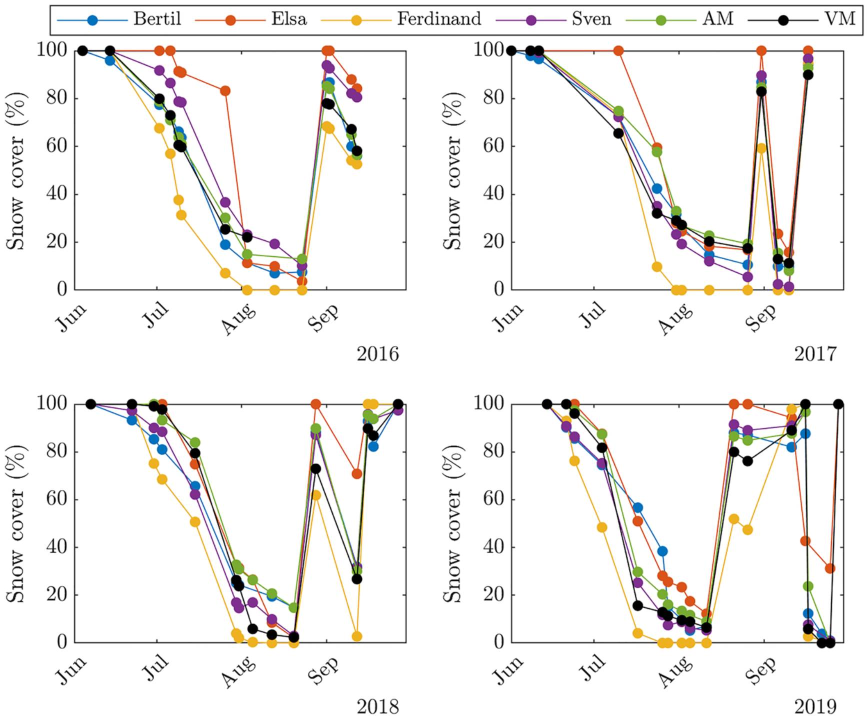

Fig. 2. Snow cover dynamics on the selected glaciers expressed as a percentage during the summer ablation seasons for the period 2016–19.

However, clear temporal differences can be distinguished on an annual scale and between glaciers. In general, the snow cover extent on the glacier surfaces started to decrease in mid-June. Usually, the ablation continued until late August or the beginning of September when the first snow fall occurred. The new snow then melted within a few days after which the already uncovered glacier surface stayed (almost) snow-free until the middle or end of September when permanent snow cover resettled. In 2017 and 2019, the snow cover extent only reached its absolute minimum on some glaciers after the first snowfall event of the ablation season, see Figure 2.

The proportion of persisting snow cover extent decreased to at least 22% on all studied glaciers (Table 2). Note that the reported highest minimum snow cover extent on any glacier was most likely <22% due to cloud cover over the Vestre Munin glacier in 2016. The snow cover disappeared completely during all years on Ferdinand glacier, which has both the lowest median elevation (420 m a.s.l.) as well as the lowest maximum elevation (540 m a.s.l.). As a result, Ferdinand was typically the first glacier to lose its snow cover completely, see Figure 2. Moreover, both Austre Munin as well as Vestre Munin glaciers were snow free in 2019 while this was almost the case for Sven glacier in all years except for 2016. Table 2 also points out that each of the studied glaciers had at least 1 year with practically none or no snow cover.

Interestingly, there is no regularity in the location of the highest yearly minimum snow cover among the glaciers (Table 2). Elsa glacier, being the highest positioned glacier of those studied, could

Table 2. Annual minimum snow cover relative to the total glacier surface area expressed as a percentage

	B	E	F	S	AM	VM
2016	7.1	3.7	0.0	10.2	13.0	**22.1**
2017	9.8	**15.8**	0.0	14.3	8.0	11.3
2018	14.8	2.2	0.0	3.0	**14.8**	2.4
2019	1.0	**12.3**	0.0	0.8	0.0	0.0
Mean	8.2	8.5	0	3.9	9.0	8.9

A complete glacier snow cover is reflected by 100% and no snow cover by 0%. Bold numbers signal the highest minimum snow cover of all glaciers during a year.

be expected to have the highest percentage of snow cover but only had the highest minimum proportion of snow-covered surface during two out of the four years studied. This underlines the highly variable nature of the snow cover. Yet, four (B, E, AM, VM) out of six glaciers had a strikingly similar 4-year average minimum snow cover extent. The position of the persisting snow cover (i.e. accumulation area) on the studied glaciers seems to be driven by a combination of altitude, aspect and terrain morphology (Fig. 3). This is well visible in the case of Bertil glacier where one of the most important accumulation zones is located on the western part of the glacier which is shaded by high mountain slopes (above 550 m a.s.l.). On the contrary, the northernmost part of the Sven glacier (exposed to the south) has only a minor accumulation zone despite the relatively high altitude (above 600 m a.s.l.).

An estimate of the number of days without snow cover on a significant part of the glacier surface could be made for each glacier during the studied years. In Table 3, the latter is defined as the mean number of days below a threshold snow cover. Ferdinand glacier clearly stands out in terms of the high number of days with a low snow cover and therefore exposed ice surface. With the exception of the small Elsa glacier for which the surface seems to be generally exposed on the least number of days, the other four glaciers are on average exposed to a similar number of days with <70% snow cover.

Discussion

The thinning of the studied glaciers, especially in the highly elevated areas (Małecki, 2016), can be explained through the combination of three key factors: (i) the continuing increase of air temperature (Nordli and others, 2014), (ii) low precipitation due to the relatively continental climate (Gjelten and others, 2016) such that increasing ablation cannot be compensated and (iii) local topography as a key factor affecting shading and direct exposure to solar radiation as well as deposition of snow during the winter. Especially the first two factors are expressed in the equilibrium line altitude (ELA) which reflects both temperature and precipitation conditions of the region. James and others

https://doi.org/10.1017/jog.2021.36 Published online by Cambridge University Press

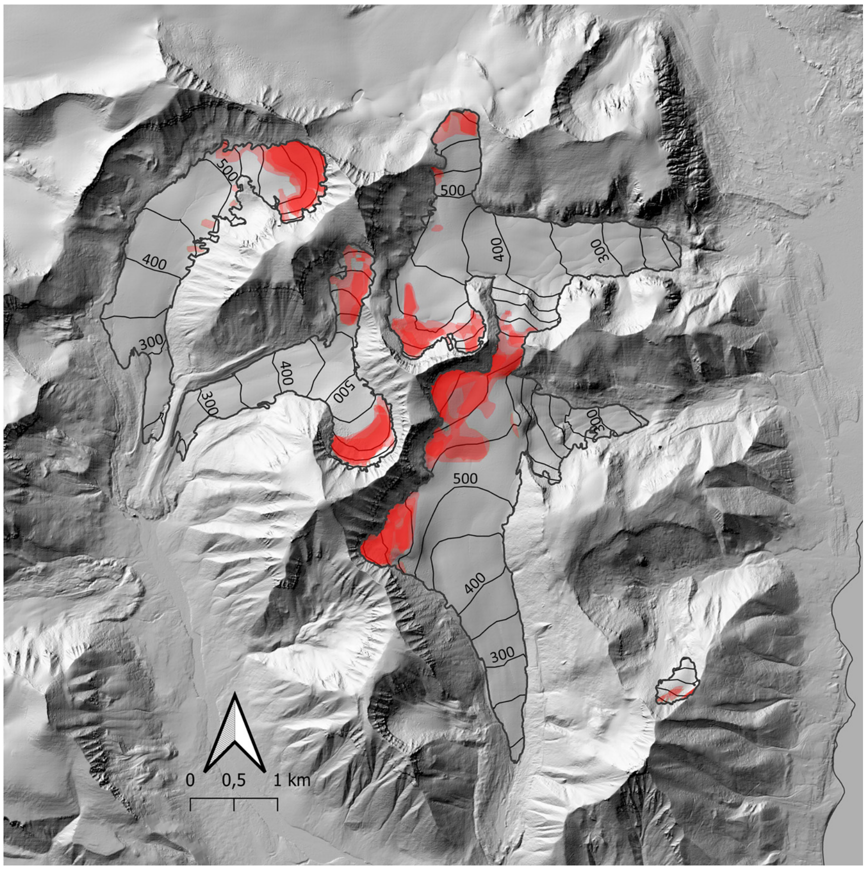

Fig. 3. Minimum snow cover extent on the selected glaciers in summer seasons 2016–19 presented on the background of the 2009 DEM; the minimum snow cover extents (red) are overlapped for each year.

Table 3. Mean estimated number of days with less than 90, 70, 50, 30 or 10% glacier snow cover

%	B	E	F	S	AM	VM
<90	95	66	91	83	85	88
<70	63	44	78	56	61	64
<50	43	35	57	45	42	44
<30	30	25	46	33	30	30
<10	10	5	34	12	2	9

The higher the number of days with a protective snow cover below a defined threshold, the longer the glacier surface was exposed to potential ice melt.

(2012) emphasized the importance of ELA for Svalbard glaciers. Even a small increase in ELA would result in extreme melting due to the hypsometric distribution of Svalbard glaciers.

With the prolongation of the melting season as a result of rising temperatures on Svalbard (Førland others, 2011), the importance of the summer glacier ablation season, and therefore the snow cover dynamics increases. The summer ablation dynamics of glaciers in the Hornsund region (southern Spitsbergen) were investigated in 2014 by Laska and others (2017) who found that 43% of the glacier area had a snow cover at the end of the ablation season. This is significantly higher than the minimum snow cover extents found on the six investigated glaciers during the 2016–19 period. In another study, Wójcik and Sobota (2020) investigated Irene glacier on the Kaffiøyra plain, northwestern Spitsbergen. Here, intense ablation was found to occur up to 400–450 m a.s.l., where no snow cover persisted. The snow cover extent at the end of the ablation season was limited to ∼20% and, like the Dicksonland glaciers in central Spitsbergen, occupied the high elevated and shaded zones. Now, despite the higher elevation of the Dicksonland glaciers, the proportion of snow cover is generally lower than on Irene glacier. This might be a result of the higher precipitation on the west coast of Svalbard (Førland others, 2011). A larger snow depth due to higher winter precipitation rates in the maritime region can potentially persist longer into the summer ablation season and will not melt completely despite the lower altitude of the glacier (100–600 m a.s.l.). The higher proportion of the snow-covered area in case of Hornsund glaciers may be attributed to a similar cause in combination with larger areal extents of the glaciers and the altitudes of up to 1200 m a.s.l. (Laska and others, 2017). The low accumulation rate is also in accordance with findings of Hagen and others (2003) who observed negative mass balances of central Svalbard glaciers up to 500–600 m a.s.l., while also being the region with the highest ELA compared to other regions of Svalbard. The overlap of the minimum snow-covered area between the years studied on the glaciers in Dicksonland is relatively large, which is in good accordance with the findings of Helfricht and others (2014). Based on this, the accumulation areas for five out of six glaciers could be delineated. No accumulation area could be determined on Ferdinand glacier. The accumulation area on Elsa glacier might also be influenced by the input of snow from avalanches originating from the above lying steep slopes. This may explain the high proportion of snow covered area in 2017 and 2019 in contrast to 2016 and 2018 when the glacier had only very small snow accumulation areas.

The lack of an accumulation zone on Ferdinand glacier reflects its low altitude and supports the findings of Procházková and others (2019) who reported the glacier to be experiencing extreme thinning. In contrast, Małecki (2016) did not report such dramatic changes in case of Ferdinand glacier. The latter is caused by a different delineation approach for the outline boundary between Ferdinand glacier and Bertil glacier. Małecki (2013, 2016) defined the Ferdinand glacier outlines based on a digital elevation model, which resulted in the Ferdinand glacier being extended with the upper parts of the neighbouring Bertil glacier. This is contradictory to the GPR profiles reported by Procházková

https://doi.org/10.1017/jog.2021.36 Published online by Cambridge University Press

and others (2019), who found only a thin ice layer between Ferdinand glacier and Bertil. Therefore, a respective boundary between both glaciers was defined and used in this study (see Fig. 1b). The ice-covered boundary south of the roche moutonée already melted in 2016/17 and bedrock is now exposed. The northern part of Ferdinand glacier had <5 m of ice thickness left in 2015 (Procházková and others, 2019).

The accumulated winter snowpack needs to decrease in depth (i.e. melt) before any retreat of the snow cover extent can be observed. Therefore, the start of the summer ablation season most likely occurred before observations of a reduction in the snow cover extent as reported in Figure 2. The actual summer melt onset (SMO) can instead be determined through microwave backscatter measurements as done by Rotschky and others (2011) for the whole of Svalbard for the period 2000–09. During this period, SMO occurred with an offset of about 2 weeks between 28 May in south Spitsbergen and 12 June in Nordaustlandet. Taking the former into account and comparing the latter with our observations, we can conclude that the snow cover extent starts to decrease during the second half of June on all glaciers after the average SMO. Once the snow cover starts to retreat, an increasing part of the glacier surface is exposed which changes the albedo and thus the surface energy balance. Laska and others (2017) reported that the highest melt rate was recorded in July, when most of the glacier ablation zone had lost its protective snow cover. Thus, the number of days at which a glacier surface potentially undergoes ice melt is dependent on (the lack of) a snow cover. In result, the number of days below a threshold snow cover, indicates the potential number of melt days on a significant part of the studied glaciers.

The classical glaciological method of using a network of ablation stakes to assess the glacier mass balance is labour-demanding. This led to the development of different automated mass balance methods (e.g. Hulth, 2010; Carturan and others, 2019). However, these methods are expensive, usually restricted to point measurements and often experience technical failures. In that view, using publicly available satellite images (e.g. Sentinel-2) can enhance our knowledge of crucial snow cover ablation dynamics with high spatial and temporal resolutions at minimum cost and high accessibility. For example, Jain and others (2011) used remote sensing techniques in combination with air temperature measurements to assess the depletion of the catchment snow cover during the ablation season. The product of such assessments can be a snow cover depletion curve which in turn can be used for hydrological modelling. In relation to this, Li and others (2015) noted that the incorporation of seasonal snow cover dynamics on a glacier's surface is crucial when modelling catchment runoff. The importance of the latter is supported by Azam and others (2019) who identified snow accumulation combined with summer ice melt as a control of catchment-wide runoff and glacier mass balance. Hence, the snow ablation dynamics as presented in this study might be used to better capture the modelled peak discharge during spring snow melt and later in summer to support the modelling of ice melt from the exposed glacier surface.

Conclusion

The six studied glaciers experienced dramatic ablation of their winter snow cover, with only a fraction persisting through the summer ablation season. The analysis of available satellite images between 2016 and 2019 revealed that all the studied glaciers are very likely experiencing major thinning on >80% of their surface area as a result of a non-persisting winter snow cover. Each of the studied glaciers had at least one year with practically none or no snow cover. Persisting snow cover is found in higher elevated zones that are favourable for major snow accumulation during winter and partly protected from direct insulation due to shading during the summer ablation period. Similarly, well-illustrated snow cover ablation dynamics were observed, while temporal and annual differences could be distinguished. Averaged estimates of the numbers of days without snow cover on a significant part of the glacier surface were made for each glacier. The (lack of) snow accumulation zones and their spatial distribution across the glacier surface could be used to explain the overall negative mass balance of the glaciers and their spatial variability. Finally, knowledge of the snow cover ablation dynamics provides valuable information not just for glaciology but can also support hydrological modelling efforts which are often confronted with a lack of in-situ measurements.

Acknowledgements. This work was supported by the Czech Science Foundation project GC20-20240S, Masaryk university project ARCTOS MU (MUNI/G/1540/2019) and Arctic Field Grant project 'Glacier mass balance – central Svalbard' (RiS ID 10903), funded by The Research Council of Norway. The logistic support of the staff of the Adam Mickiewicz University Polar Station is highly appreciated as well. Our gratitude also belongs to Florian von Ah and Florian Großmann for the proof reading and to Steve Riley for the language editing.

References

Ai S and 5 others (2014) Topography, ice thickness and ice volume of the glacier Pedersenbreen in Svalbard, using GPR and GPS. *Polar Research* **33**(1), 18533. doi: 10.3402/polar.v33.18533.

Ambrožová K and Láska K (2017) Air temperature variability in the vertical profile over the coastal area of Petuniabukta, central Spitsbergen. *Polish Polar Research* **38**, 41–60. doi: 10.1515/popore-2017-0004.

Azam MF and 7 others (2019) Snow and ice melt contributions in a highly glacierized catchment of Chhota Shigri glacier (India) over the last five decades. *Journal of Hydrology* **574**, 760–773. doi: 10.1016/j.jhydrol.2019.04.075.

Carturan L, Cazori F, Dalla Fontana G and Zanoner T (2019) Automatic measurement of glacier ice ablation using thermistor strings. *Journal of Glaciology* **65**(250), 188–194. doi: 10.1017/jog.2018.103.

Forłand E, Benestad R, Hanssen-Bauer I, Haugen J and Engen-Skaugen T (2011) Temperature and precipitation development at Svalbard 1900–2100. *Advances in Meteorology* **2011**, 893790. doi: 10.1155/2011/893790.

Gallet JC and 9 others (2018) *Snow research in Svalbard: current status and knowledge gaps. State of Environmental Science in Svalbard (SESS) report 2018.* SIOS Svalbard.

Gjelten HM and 9 others (2016) Air temperature variations and gradients along the coast and fjords of western Spitsbergen. *Polar Research* **35**(1), 29878. doi: 10.3402/polar.v35.29878.

Hagen JO, Melvold K, Pinglot F and Dowdeswell JA (2003) On the net mass balance of the glaciers and ice caps in Svalbard, Norwegian Arctic. *Arctic, Antarctic, and Alpine Research* **35**(2), 264–270. doi: 10.1657/1523-0430(2003)035[0264:OTNMBO]2.0.CO;2.

Helfricht K, Schöber J, Schneider K, Sailer R and Kuhn M (2014) Interannual persistence of the seasonal snow cover in a glacierized catchment. *Journal of Glaciology* **60**(223), 889–904. doi: 10.3189/2014JoG13J197.

Hulth J (2010) Using a draw-wire sensor to continuously monitor glacier melt. *Journal of Glaciology* **56**(199), 922–924. doi: 10.3189/002214310794457290.

Humlum O, Instanes A and Sollid JL (2003) Permafrost in Svalbard: a review of research history, climatic background and engineering challenges. *Polar Research* **22**(2), 191–215. doi: 10.3402/polar.v22i2.6455.

Jaedicke C and Gauer P (2005) The influence of drifting snow on the location of glaciers on western Spitsbergen, Svalbard. *Annals of Glaciology* **42**, 237–242. doi: 10.3189/172756405781812628.

Jain S, Thakural L, Singh R, Lohani AK and Mishra S (2011) Snow cover depletion under changed climate with the help of remote sensing and temperature data. *Natural Hazards* **58**, 891–904. doi: 10.1007/s11069-010-9696-1.

James TD and 5 others (2012) Observations of enhanced thinning in the upper reaches of Svalbard glaciers. *The Cryosphere* **6**(6), 1369–1381. doi: 10.5194/tc-6-1369-2012.

Kavan J (2020) Early twentieth century evolution of Ferdinand glacier, Svalbard, based on historic photographs and structure-from-motion technique. *Geografiska Annaler: Series A, Physical Geography* **102**(1), 57–67. doi: 10.1080/04353676.2020.1715124.

Lapazaran J and 6 others (2013) Ice volume changes (1936–1990–2007) and ground-penetrating radar studies of Ariebreen, Hornsund, Spitsbergen. *Polar Research* **32**, 11068. doi: 10.3402/polar.v32i0.

Laska M, Barzycka B and Luks B (2017) Melting characteristics of snow cover on tidewater glaciers in Hornsund fjord, Svalbard. *Water* **9**, 804.

Li H and 5 others (2015) Integrating a glacier retreat model into a hydrological model – case studies of three glacierised catchments in Norway and Himalayan region. *Journal of Hydrology* **527**, 656–667.

Małecki J (2013) Elevation and volume changes of seven Dickson Land glaciers, Svalbard, 1960–1990–2009. *Polar Research* **32**(1), 18400. doi: 10.3402/polar.v32i0.18400.

Małecki J (2015) Snow accumulation on a small high-arctic glacier Svenbreen: variability and topographic controls. *Geografiska Annaler Series A Physical Geography* **97**, 809–817. doi: 10.1111/geoa.12115.

Małecki J (2016) Accelerating retreat and high-elevation thinning of glaciers in central Spitsbergen. *The Cryosphere* **10**(3), 1317–1329. doi: 10.5194/tc-10-1317-2016.

Mallinson L, Swift DA and Sole A (2019) Proglacial icings as indicators of glacier thermal regime: ice thickness changes and icing occurrence in Svalbard. *Geografiska Annaler: Series A, Physical Geography* **101**(4), 334–349. doi: 10.1080/04353676.2019.1670952.

Marlin C and 6 others (2017) Change in geometry of a high Arctic glacier from 1948 to 2013 (Austre Lovénbreen, Svalbard). *Geografiska Annaler: Series +A, Physical Geography* **99**(2), 115–138. doi: 10.1080/04353676.2017.1285203.

Martín-Moreno R, Álvarez FA and Hagen JO (2017) 'Little Ice Age' glacier extent and subsequent retreat in Svalbard archipelago. *The Holocene* **27**(9), 1379–1390. doi: 10.1177/0959683617693904.

Nilsen F, Cottier F, Skogseth R and Mattsson S (2008) Fjord-shelf exchanges controlled by ice and brine production: the interannual variation of atlantic water in Isfjorden, Svalbard. *Continental Shelf Research* **28**(14), 1838–1853, ISSN 0278-4343. doi: 10.1016/j.csr.2008.04.015.

Noël B and 10 others (2020) Low elevation of Svalbard glaciers drives high mass loss variability. *Nature Communications* **11**, 4597. doi: 10.1038/s41467-020-18356-1.

Nolin AW (2010) Recent advances in remote sensing of seasonal snow. *Journal of Glaciology* **56**(200), 1141–1150. doi: 10.3189/002214311796406077.

Nordli O, Przybylak R, Ogilvie AE and Isaksen K (2014) Long-term temperature trends and variability on Spitsbergen: the extended Svalbard airport temperature series, 1898–2012. *Polar Research* **33**(1), 21349. doi: 10.3402/polar.v33.21349.

NPI (2021) Seasonal temperatures for Svalbard airport. environmental monitoring of Svalbard and Jan Mayen (mosj). Available at https://www.mosj.no/en/climate/atmosphere/temperature-precipitation.html (Accessed 7 January 2021).

Nuth C, Kohler J, Aas H, Brandt O and Hagen J (2007) Glacier geometry and elevation changes on Svalbard (1936–90): a baseline dataset. *Annals of Glaciology* **46**, 106–116. doi: 10.3189/172756407782871440.

Procházková B, Engel Z and Tomíček J (2019) Geometric changes of three glaciers in Dickson land, Central Spitsbergen, during the period 1990–2015. *Polar Science* **20**, 129–135, ISSN 1873-9652. doi: 10.1016/j.polar.2019.05.004.

Przybylak R and 10 others (2014) Spatial distribution of air temperature on Svalbard during 1 year with campaign measurements. *International Journal of Climatology* **34**(14), 3702–3719. doi: 10.1002/joc.3937.

Rachlewicz G, Szczuciński W and Ewertowski M (2007) Post-"little ice age" retreat rates of glaciers around Billefjorden in central Spitsbergen, Svalbard. *Polish Polar Research* **28**, 159–186.

Rotschky G, Schuler T, Haarpaintner J, Kohler J and Isaksson E (2011) Spatio-temporal variability of snowmelt across Svalbard during the period 2000–08 derived from quikscat/seawinds scatterometry. *Polar Research* **30**, 5963. doi: 10.3402/polar.v30i0.5963.

Schuler TV and 12 others (2020) Reconciling Svalbard glacier mass balance. *Frontiers in Earth Science* **8**, 156, ISSN 2296-6463 doi: 10.3389/feart.2020.00156.

Szczuciński W, Zajączkowski M and Scholten J (2009) Sediment accumulation rates in subpolar fjords – impact of post-Little Ice Age glaciers retreat, Billefjorden, Svalbard. *Estuarine, Coastal and Shelf Science* **85**(3), 345–356, ISSN 0272-7714. doi: 10.1016/j.ecss.2009.08.021.

Turpin O, Caves R, Ferguson R and Johansson B (2000) Verification of simulated snow cover in an Arctic basin using satelite-derived snow-cover maps. *Annals of Glaciology* **31**, 391–396. doi: 10.3189/172756400781819932.

Wójcik KA and Sobota I (2020) Spatial and temporal changes in ablation, distribution and evolution of glacial zones on Irenebreen, a small glacier of the High Arctic, Svalbard. *Polar Science* **23**, 100503. doi: 10.1016/j.polar.2020.100503.

APPENDIX

Table 4. Dates of origin of the Sentinel-2 images used for evaluation of snow coverage on the studied glaciers

2016	2017	2018	2019
04.06	01.06	07.06	14.06
14.06	08.06	22.06	21.06
02.07	11.06	30.06	24.06
06.07	10.07	03.07	04.07
09.07	24.07	15.07	17.07
10.07	31.07	30.07	26.07
26.07	02.08	31.07	28.07
03.08	12.08	12.08	02.08
13.08	26.08	20.08	05.08
23.08	31.08	28.08	11.08
01.09	06.09	12.09	21.08
02.09	10.09	16.09	26.08
10.09	17.09	18.09	11.09
12.09		27.09	16.09
			17.09
			22.09
			25.09
			28.09

https://doi.org/10.1017/jog.2021.36 Published online by Cambridge University Press